# Generation of Kerr squeezed light and its application to interferometry

Der Naturwissenschaftlichen Fakultät
der Friedrich-Alexander-Universität
Erlangen-Nürnberg
zur
Erlangung des Doktorgrades Dr. rer. nat.

vorgelegt von
**Nikolay Kalinin**
aus Nischni Nowgorod

Als Dissertation genehmigt
von der Naturwissenschaftlichen Fakultät
der Friedrich-Alexander-Universität Erlangen-Nürnberg

Tag der mündlichen Prüfung: 24. April 2024

Gutachter: Prof. Dr. Gerd Leuchs
Prof. Dr. Stephan Götzinger
Prof. Dr. Markus Oberthaler

## Abstract

The quantum nature of light limits the precision with which some of its characteristics can be defined. A variety of nonclassical states exists which, in principle, allows to lower some of these limits. Squeezed light states are among the simplest of these nonclassical states, and yet they are very effective. In this thesis, we investigate the generation of squeezed states using the Kerr effect in fibers, and the application of these states to interferometry. In particular, we develop a novel setup for the generation of polarization-squeezed states which is very stable and does not require any active feedback loop. We investigate the range of possible parameters of this system to optimize squeezing, both experimentally and numerically. We suggest a way to apply Kerr squeezed states to interferometry, and implement it in the experiment. For the first time, we demonstrate that it is indeed possible to enhance the sensitivity of an interferometer beyond the shot noise limit with the use of such Kerr squeezed states.

## Zusammenfassung

Die Quantennatur des Lichts begrenzt die Genauigkeit, mit der einige seiner Eigenschaften definiert werden können. Es gibt eine Vielzahl nichtklassischer Zustände, die es grundsätzlich ermöglichen, einige dieser Begrenzungen zu überwinden. Gequetschte Lichtzustände gehören zu den einfachsten dieser nichtklassischen Zustände und sind dennoch sehr effektiv. In dieser Arbeit untersuchen wir die Erzeugung gequetschter Zustände mithilfe des Kerr-Effekts in Fasern und ihre Anwendung in der Interferometrie. Insbesondere entwickeln wir einen neuartigen Aufbau zur Erzeugung polarisationsgequetschter Zustände, der robust ist und keine Stabilisierung zum Beispiel durch eine aktive Rückkopplungsschleife erfordert. Wir variieren die relevanten Parameter dieses Systems, um das Quetschen sowohl experimentell als auch numerisch zu optimieren. Wir schlagen eine Möglichkeit vor, Kerr-gequetschte Zustände auf die Interferometrie anzuwenden und im Experiment zu implementieren. Zum ersten Mal zeigen wir, dass es tatsächlich möglich ist, die Empfindlichkeit eines Interferometers durch Verwendung solcher Kerr-gequetschen Zustände über die Schrotrauschgrenze hinaus zu steigern.

## Acknowledgments

This thesis is a product of a series of sudden falls caused by the most unimaginable circumstances, and uplifting moments powered by the kindness of the people I hold dear. I would like to express my special gratitude to two individuals, without whom this thesis would not exist.

Thank you, Alexey Andrianov, for being a great supervisor since my first days in the lab and all the way during my bachelor's, master's, and doctorate studies. Your constant encouragement, both at work and beyond, has always been a great motivation for me. Thank you for being my guide in scientific work; I have learned a lot from you.

Thank you, Gerd Leuchs, not only for your advice and guidance throughout the years, but also for your kindness, understanding, and support that enabled me to finish my thesis at MPL at the time the initial plan was becoming less and less feasible. I can't imagine a more thoughtful advisor than you.

Last but not least, I give my heartfelt thanks to my friends, colleagues, and family for the tremendous support I received while working on the thesis. Thank you, Спасибо, Danke!

# Contents

# Part I

# Scientific context

# Chapter 1

# Introduction

The invention of the laser was, undoubtedly, one of the most important technological advances of the $20^{\text{th}}$ century. Only with strong coherent radiation provided by lasers people started to truly control light, exploring its unique properties in a wide variety of applications. However, there are limits to which certain parameters of light can be precisely adjusted. In experiments, the limiting factors usually include tiny misalignments, losses, scattering, as well as technical noise in the source laser or in the setup. However, when these problems are resolved, or their effect is reduced to a negligible value, there is one more contributing factor — the quantum nature of light.

Long before the first experimental demonstration of a laser, Heisenberg's uncertainty principle was found to limit the precision with which complementary variables of a quantum system can be defined. Most known is the form that the position and speed of a particle couldn't be simultaneously measured with precision. The principle is universal and applies to different variables of a light field as well. Quantum states that are the most appropriate analogue of a perfect classical wave — the coherent states [1] — have a symmetric distribution of uncertainty over complementary variables. These states define the so-called shot-noise limit (SNL) for the measurement precision, which applies as long as no non-classical light sources are used.

Fortunately, it is possible to overcome the SNL with the use of specifically designed quantum states — the so-called squeezed states [2]. After lengthy theoretical and experimental work, such states were first observed in a groundbreaking experiment by Slusher et al. in 1985 [3]. Now, more than 35 years later, squeezed state generation is already used as a tool in

much larger experiments, such as gravitational waves detection [4] or optical quantum computing [5]. On the other hand, the search for a more compact, robust, and efficient source of squeezed light continues [6–8].

This work investigates the Kerr nonlinearity in optical fibers as a means of squeezed light generation. While this system was among the first where squeezing was observed, it is nowadays used less frequently than its competitors. This is due to a number of challenges, some of which are discussed and solved in this work. The following structure of this thesis is as follows. In Chapter 2, necessary theoretical foundations are discussed. Chapter 3 is devoted to experimental demonstrations of Kerr squeezing in fibers and the role of a new setup implemented in this work. More details on the setup and supporting calculations can be found in the following works:

- Kalinin, N., Dirmeier, T., Sorokin, A. A., Anashkina, E. A., Sánchez-Soto, L. L., Corney, J. F., Leuchs, G., Andrianov, A. V., Observation of Robust Polarization Squeezing via the Kerr Nonlinearity in an Optical Fiber. Adv Quantum Technol. 6, 2200143, 2023. 10.1002/qute.202200143.

- Andrianov, A. V., Kalinin, N. A., Sorokin, A. A., Anashkina, E. A., Sánchez-Soto, L. L., Corney, J. F., and Leuchs, G., Optimizing the generation of polarization squeezed light in nonlinear optical fibers driven by femtosecond pulses, Opt. Express 31, 765, 2023. 10.1364/OE.481195.

- Sorokin, A. A., Leuchs, G., Corney, J. F., Kalinin, N. A., Anashkina, E. A., and Andrianov, A. V., Towards Quantum Noise Squeezing for 2-Micron Light with Tellurite and Chalcogenide Fibers with Large Kerr Nonlinearity, Mathematics 10 (19), 3477, 2022. 10.3390/math10193477.

In Chapter 4, approaches to interferometer sensitivity enhancement are discussed, and a novel way that uses Kerr squeezing is introduced. More details about this approach can be found in the following work.

- Kalinin, N., Dirmeier, T., Sorokin, A. A., Anashkina, E. A., Sánchez-Soto, L. L., Corney, J. F., Leuchs, G., Andrianov, A. V., Quantum-enhanced interferometer using Kerr squeezing. Nanophotonics 12 (14), 2945, 2023. 10.1515/nanoph-2023-0032.

In Chapter 5, conclusion and outlook are given.

# Chapter 2

# Theoretical foundations

## 2.1 Optical Kerr effect

The Kerr effect is the change of the refraction index of a medium, proportional to the second power of the electric field. In amorphous materials, or crystals whose structure is centrally-symmetrical, the quadratic (linear in electric field) nonlinearity cannot exist, and thus the cubic Kerr nonlinearity prevails. Concerning applications, one of the most important media in which the Kerr nonlinearity dominates are optical fibers, typically made of amorphous glasses. The Kerr effect can be caused by an external electric field, as well as by self-action of the electric field of a propagating optical pulse. In the latter case, the effect is often called the optical Kerr effect. In the following, the optical Kerr effect in glass fibers is considered since it is the most important one for this work.

When pulses of long enough duration (more than 10 ps) propagate down an optical fiber, the Kerr effect can be considered instantaneous [9], and then the refraction index can be represented in the following form:

$$n(\vec{r}, t) = n_0 + n_2 I(\vec{r}, t), \tag{2.1}$$

where $n_0$ is the refraction index in the absence of the electric field, $I(\vec{r}, t)$ is the intensity of the radiation, and $n_2$ is a parameter of the medium called the second-order nonlinear refractive index. When pulses propagate in optical fibers, the Kerr effect plays a key role in many nonlinear interactions. In particular, it allows for soliton propagation in the region of anomalous dispersion. It can also affect the transverse mode distribution in the fiber, leading to extreme effects such as self-focusing inside the fiber core.

However, for single mode fibers and at the power levels considered in this work, the transversal nonlinear effects are negligible.

In the classical description of a single mode of light, the Kerr effect leads to an amplitude-dependent shift of the absolute phase of the light. In Fig. 2.1, the effect is shown in quadrature space, where $|\alpha|$ is the amplitude, and $\phi = \arg\alpha$ is the phase of the light, while

$$\begin{aligned} X_1 &= \frac{1}{2}(\alpha + \alpha^*) = |\alpha| \cos\phi, \\ X_2 &= \frac{i}{2}(\alpha^* - \alpha) = |\alpha| \sin\phi \end{aligned} \tag{2.2}$$

are the quadrature variables. Since the absolute phase usually does not play a significant role, the most important effects appear when pulse propagation is considered, and the intrapulse phase relation is becoming important.

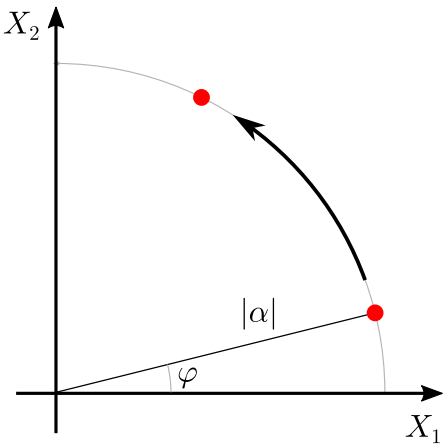


**Figure 2.1:** Classical action of the Kerr effect in the quadrature space.

On the contrary, in the quantum description, even a single mode state is affected by the Kerr effect. In this picture, it's not possible to determine amplitude and phase exactly, and we must consider that a light state representation in quadrature space has some uncertainty area. Then, the Kerr effect changes the shape of that uncertainty area by introducing some correlation between amplitude and phase, as shown in Fig. 2.2. In order to properly assess this effect, however, we must first introduce some quantum formalism to describe various light states.

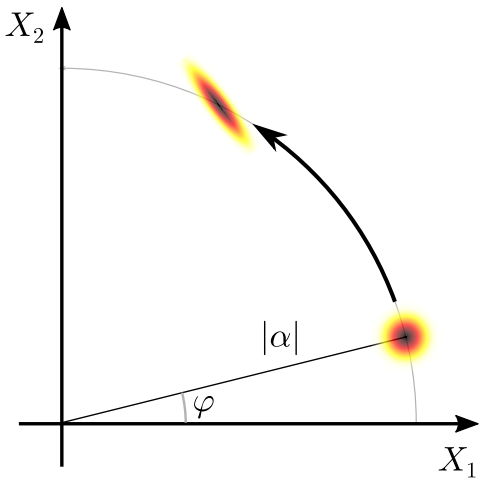


**Figure 2.2:** The quantum action of the Kerr effect in the quadrature space (or phase space).

## 2.2 Quantum mode description

In classical electrodynamics, all electromagnetic fields can be represented as a combination of specific modes, each having well-defined spatial and spectral shapes and a well-defined polarization. Each mode can be excited to an arbitrary energy level. We will pay attention to only one of these modes, which, as per standard quantization, can be represented by a pair of annihilation $\hat{a}$ and creation $\hat{a}^\dagger$ operators in the quantum description.

These operators obey the standard commutation relation

$$\left[\hat{a}, \hat{a}^\dagger\right] = 1, \tag{2.3}$$

while the number of photons in the mode is represented by the number operator $\hat{n} = \hat{a}^\dagger\hat{a}$, and the energy operator, or the Hamiltonian, for the mode is

$$\hat{H} = \hbar\omega(\hat{n} + \frac{1}{2}), \tag{2.4}$$

where $\omega$ is the mode frequency. This is formally analogous to a harmonic oscillator. The eigenvalues of the number operator are known to be non-negative integer numbers, and thus the possible energy levels are separated by $\hbar\omega$. The states having well-defined energy (or, equivalently, photon

number) are the number states

$$|n\rangle = \frac{\hat{a}^{\dagger n}}{\sqrt{n!}} |0\rangle , \tag{2.5}$$

where $|0\rangle$ is the vacuum state. These states do not have a specific optical phase, are far from the states produced by typical lasers, and are difficult to generate for $n > 1$. Of course, phase and energy (or amplitude) can not be well-defined simultaneously, so some trade-off in the uncertainty of these two values is required. It turns out that the closest analog to a perfect classical wave, and also to the states produced by ideal noise-free lasers (unless some additional arrangements are made, see [10, 11]) are the so-called coherent states

$$|\alpha\rangle = \exp\Big(\alpha\hat{a}^\dagger - \alpha^*\hat{a}\Big) |0\rangle , \tag{2.6}$$

where $\alpha$ is the complex amplitude of the corresponding classical state. We can see the relation between the classical and quantum states by calculating the mean number of photons

$$\langle\alpha|\hat{n}|\alpha\rangle = |\alpha|^2, \tag{2.7}$$

and by introducing the quantum quadrature operators $\hat{X}_1 = \frac{1}{2}(\hat{a} + \hat{a}^\dagger)$ and $\hat{X}_2 = \frac{i}{2}(\hat{a}^\dagger - \hat{a})$, which are the quantum equivalent of the classical quadrature parameters. Then, the mean values

$$\begin{aligned} \langle\alpha|\hat{X}_1|\alpha\rangle &= \operatorname{Re}\alpha, \\ \langle\alpha|\hat{X}_2|\alpha\rangle &= \operatorname{Im}\alpha \end{aligned} \tag{2.8}$$

coincide with the classical ones in Eq. (2.2).

The quadrature operators play an important role in understanding squeezed states of light. The commutation relation is $\left[\hat{X}_1, \hat{X}_2\right] = \frac{i}{2}$, and thus the two values can not be well-defined simultaneously. Instead, we have the uncertainty relation

$$\operatorname{Var}\left(\hat{X}_1\right) \operatorname{Var}\left(\hat{X}_2\right) \geq \frac{1}{16}, \tag{2.9}$$

where $\operatorname{Var}\left(\hat{X}_i\right)$ denotes the variance $\left\langle \hat{X}_i^2 \right\rangle - \left\langle \hat{X}_i \right\rangle^2$. More generally, for an arbitrary quadrature operator $\hat{X}(\theta) = \cos(\theta)\hat{X}_1 + \sin(\theta)\hat{X}_2$ the uncertainty relation reads

$$\operatorname{Var}\left(\hat{X}(\theta)\right) \operatorname{Var}\left(\hat{X}\left(\theta + \frac{\pi}{2}\right)\right) \geq \frac{1}{16}. \tag{2.10}$$

We can show that for a coherent state $|\alpha\rangle$ this limit is reached, and moreover, the variance does not depend on $\theta$:

$$\mathrm{Var}\left(\hat{X}(\theta)\right) = \frac{1}{4}. \tag{2.11}$$

This inequality is known as the shot noise limit[1] (SNL). We can now picture the coherent states in phase space spanned by the $X_1$ and $X_2$ axes as a Gaussian distribution with a circular contour line at half the maximum value centered at the point $(\mathrm{Re}\,\alpha, \mathrm{Im}\,\alpha)$ (see Fig. 2.2). This representation is called the phasor diagram [12], although we have not yet defined the specific function to be plotted. It turns out that since it is not possible to observe $\hat{X}_1$ and $\hat{X}_2$ simultaneously, it is also not possible to define any probability amplitude function of these two parameters to represent the state. Several two-dimensional quasi-probability functions have been used to represent the state on the $\hat{X}_1$–$\hat{X}_2$ plane, one of them is the Wigner function $W(X_1, X_2) = W(\beta)$, where $\beta = X_1 + iX_2$. For an arbitrary state $|\Psi\rangle$, the Wigner function is defined as [13–16]

$$\begin{aligned} W_{|\Psi\rangle}(\beta) &= \frac{2}{\pi}\,\langle\Psi|\hat{D}(\beta)\hat{\Pi}\hat{D}(-\beta)|\Psi\rangle\,, \quad \text{where} \\ \hat{D}(\beta) &= \exp\Big(\beta\hat{a}^\dagger - \beta^*\hat{a}\Big), \quad \text{and} \\ \hat{\Pi}\,|n\rangle &= (-1)^n\,|n\rangle \quad \text{for any number state}\,|n\rangle\,. \end{aligned} \tag{2.12}$$

The Wigner function of the coherent state $|\alpha\rangle$ is a symmetric Gaussian function with unitary width:

$$W_{|\alpha\rangle}(\beta) = \frac{2}{\pi}e^{-2|\alpha-\beta|^2}, \tag{2.13}$$

and with a contour line at half height similar to what we depict in Fig. 2.2. We can think of the plot of the Wigner function as of a classical phasor diagram as long as it remains non-negative, which is the case for a coherent state. The Wigner function and its motion equation are well-studied, Section 2.5 discusses the relevant results.

## 2.3 Squeezed states

Although the uncertainty relation Eq. (2.10) holds for every possible light state, the balance between the variances of two orthogonal quadrature operators can be different. It is possible that for a specific angle $\theta_{\mathrm{sq}}$, the

[1] Some authors define the quadrature operators without the $\frac{1}{2}$ factor. Then, the SNL variance is 1.

fluctuations are below $\frac{1}{4}$, i. e.

$$\mathrm{Var}\left(\hat{X}(\theta_{\mathrm{sq}})\right) < \frac{1}{4} < \mathrm{Var}\left(\hat{X}\left(\theta_{\mathrm{sq}} + \frac{\pi}{2}\right)\right). \tag{2.14}$$

Such a state is called a squeezed state. Squeezed states are important instruments in modern quantum optics; they are being investigated in an increasing number of applications. In some of them, squeezed states replace traditionally used coherent states and thus improve the results quantitatively, e. g. in telecommunication [17] or precision measurements [4]. In some areas, e. g., continuous variable quantum computing and communication, qualitatively new results have been achieved [18,19], that would be impossible to get using coherent light. This is a consequence of two important properties of a squeezed state. The first property is the reduction of the variation itself: if only the $\hat{X}(\theta_{\mathrm{sq}})$ parameter is observed, the level of quantum noise is smaller than what we can get with a coherent state. The second one is that the squeezed state gets degraded if any loss is introduced and only retains all its quantum properties when fully transmitted. This has clear implications in quantum communications.

Squeezed states can be classified depending on the angle $\theta_{\mathrm{sq}}$ of the least fluctuations. Without loss of generality, we can assume the absolute phase of the state to be 0, i. e. $\left\langle \hat{X}_2 \right\rangle = 0$. Then, if $\theta_{\mathrm{sq}} = 0$, the state is said to be amplitude-squeezed, and the reduction of quantum noise could be clearly seen in direct detection of such light. If $\theta_{\mathrm{sq}} = \frac{\pi}{2}$, the state is phase-squeezed. The general case of arbitrary $\theta_{\mathrm{sq}}$ is the quadrature-squeezed light. A special case of a squeezed state is squeezed vacuum, where the average amplitude is zero: $\left\langle \hat{X}_1 \right\rangle = \left\langle \hat{X}_2 \right\rangle = 0$.

There are various ways to generate squeezed states, and all of them are related to some kind of nonlinear interaction. The two most known ways are the parametric down-conversion process, in which a vacuum coherent state is parametrically amplified in a $\chi^{(2)}$ medium to produce a squeezed vacuum state [20], and the self-action of a bright coherent state in a $\chi^{(3)}$ medium, producing a quadrature-squeezed light with non-zero mean amplitude. The Kerr effect enables the latter process. To the free Hamiltonian Eq. (2.4), the Kerr interaction term is introduced as [21]

$$\hat{H}_K = \hbar\chi \hat{a}^{\dagger 2}\hat{a}^2, \tag{2.15}$$

where $\chi$ is a real coefficient proportional to the nonlinear refractive index $n_2$. If an initially coherent light state $|\alpha\rangle$ propagates in such a medium, the

light state becomes

$$|\alpha, \kappa\rangle = \exp\left(-i\kappa\hat{a}^{\dagger 2}\hat{a}^2\right)|\alpha\rangle\,, \tag{2.16}$$

where $\kappa$ is the coefficient proportional to $\chi$ and the length of the medium. In the approximation of $\kappa \ll 1$, which is usually true in experiments, the Wigner function of this state is an asymmetric Gaussian function, whose contour in phase space is an ellipse, tilted with respect to the vector connecting the origin and the center of the ellipse (Fig. 2.2). It was first shown in [22] that this state can be quadrature-squeezed. Detailed calculations can be found in [23, 24].

The squeezing angle $\theta_{\text{sq}}$ of a Kerr-squeezed state in fiber experiments is usually between one and twenty degrees. Using direct detection alone, squeezing in such states is not revealed because the variance of the amplitude quadrature is not modified. This is due to the fact that the Kerr Hamiltonian Eq. (2.15) preserves the number of photons, and thus the photon statistics in a Kerr-squeezed state stays Poissonian. To detect a fairly dim quadrature-squeezed signal, a homodyne detection technique could be utilized, which allows one to measure the variances for an arbitrary angle $\theta$. However, the local oscillator should be much brighter than the signal [25]. This is usually unfeasible for Kerr squeezing because it relies on the already high intensity of the signal necessary to squeeze the quantum state. Therefore, a number of techniques have been invented to instead transform quadrature-squeezing to amplitude squeezing, which is directly detectable, or to a vacuum-squeezed state and detect it with a local oscillator. These include, for example, reflecting the squeezed state on an off-resonance cavity [26, 27], using in addition a $\chi^{(2)}$ squeezing stage [28, 29], or displacing the state in the phase space using a coherent [21, 30] or another Kerr-squeezed [31] state. Another approach is to combine two Kerr-squeezed states in orthogonal polarization modes to generate a polarization-squeezed state [32, 33], which is discussed in the next section.

## 2.4 Polarization squeezing

Following [34, 35], we now consider two orthogonal polarization modes of light sharing the same spatial and frequency mode. We define the quantum counterparts of the classical [36] Stokes operators

$$\begin{aligned} \hat{S}_0 &= \hat{a}^\dagger\hat{a} + \hat{b}^\dagger\hat{b}, \qquad & \hat{S}_1 &= \hat{a}^\dagger\hat{a} - \hat{b}^\dagger\hat{b}, \\ \hat{S}_2 &= \hat{a}^\dagger\hat{b} + \hat{b}^\dagger\hat{a}, \qquad & \hat{S}_3 &= i(\hat{b}^\dagger\hat{a} - \hat{a}^\dagger\hat{b}), \end{aligned} \tag{2.17}$$

where $\hat{a}$ and $\hat{b}$ are the annihilation operators for the two modes. Due to non-zero commutator of any pair of $\hat{S}_1$, $\hat{S}_2$, $\hat{S}_3$, there are several uncertainty relations [37]:

$$\mathrm{Var}\left(\hat{S}_i\right)\mathrm{Var}\left(\hat{S}_j\right) \geq \left|\epsilon_{ijk}\left\langle\hat{S}_k\right\rangle\right|^2, \tag{2.18}$$

where $\epsilon_{ijk}$ is the Levi-Civita symbol. When the mean polarization state is circular: $\left\langle\hat{S}_1\right\rangle = \left\langle\hat{S}_2\right\rangle = 0$, $\left\langle\hat{S}_3\right\rangle = \left\langle\hat{S}_0\right\rangle$, the only non-trivial uncertainty relation reads

$$\mathrm{Var}\left(\hat{S}_1\right)\mathrm{Var}\left(\hat{S}_2\right) \geq \left\langle\hat{S}_3\right\rangle^2. \tag{2.19}$$

We will restrict ourselves to the case of circular mean polarization in the following. We define a unitary linear combination of Stokes parameters $\hat{S}(\theta) = \cos(\theta)\hat{S}_1 + \sin(\theta)\hat{S}_2$, for which the uncertainty relation reads

$$\mathrm{Var}\left(\hat{S}(\theta)\right)\mathrm{Var}\left(\hat{S}\left(\theta+\frac{\pi}{2}\right)\right) \geq \left\langle\hat{S}_3\right\rangle^2, \tag{2.20}$$

similar to Eq. (2.10). When the light is in a coherent state in both modes, the equality in Eq. (2.20) is reached, and $\Delta^2 S(\theta)$ is independent on $\theta$. A light state is polarization-squeezed, if there exists an angle $\theta_{\mathrm{sq}}$, such that

$$\mathrm{Var}\left(\hat{S}(\theta_{\mathrm{sq}})\right) < \left|\left\langle\hat{S}_3\right\rangle\right| < \mathrm{Var}\left(\hat{S}\left(\theta_{\mathrm{sq}}+\frac{\pi}{2}\right)\right). \tag{2.21}$$

Here, again, $\theta_{\mathrm{sq}}$ is the squeezing angle. Note that a polarization-squeezed state is a two-mode state, composed of two single-mode squeezed states, which shows quantum entanglement in an appropriately chosen basis [38, 39].

Quantum polarization states are conveniently pictured in Poincaré space [35]. In general, the Wigner function is defined in the 3D space of $S_1$, $S_2$, $S_3$; however, for many applications, the total intensity $S_1^2 + S_2^2 + S_3^2$ does not play a role. Thus, often only a projection of the Wigner function on a Poincaré sphere is plotted. In Fig. 2.3, a coherent state and a squeezed state are shown. The contour line of a coherent state is a circle, while the one of a squeezed state is an ellipse, the minor axis of which is smaller than the diameter of the circle. When a linear combination of Stokes parameters oriented parallel to this minor axis is measured, a reduction of noise is observed.

In an experiment, it is fairly straightforward to arrange for a measurement of any linear combinations of the $\hat{S}_1$, $\hat{S}_2$, $\hat{S}_3$ Stokes parameters. A single Stokes parameter, typically $\hat{S}_1$, can be measured with a fixed polarizing beamsplitter and a pair of balanced detectors. With the use of several

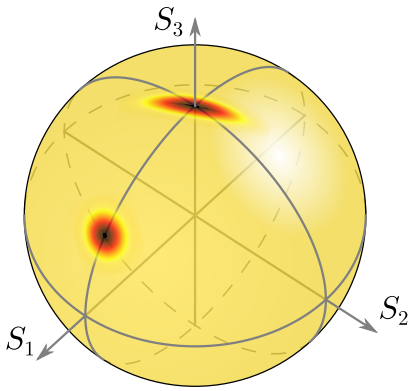


**Figure 2.3:** A coherent state of an elliptical mean polarization and a squeezed state of circular mean polarization on a Poincaré sphere.

waveplates, the measurement of any linear combination can be translated into measurements of $\hat{S}_1$, see Section 3.2. The commuting parameter $\hat{S}_0$, which is equal to the total number of photons in two modes, is also simultaneously detected. However, simultaneous detection of multiple linear combinations of $\hat{S}_1$, $\hat{S}_2$, $\hat{S}_3$ is associated with a noise penalty [40, 41].

## 2.5 Numerical modeling

The main equation describing the classical evolution of light pulses in a single-mode optical fiber is the well-known nonlinear Schrödinger equation (NLSE). In its simplest form, it reads [9]

$$\frac{\partial A}{\partial z} + \beta_1 \frac{\partial A}{\partial t} + \frac{i\beta_2}{2}\frac{\partial^2 A}{\partial t^2} + \frac{\alpha}{2}A = i\gamma|A|^2 A, \tag{2.22}$$

where $A$ is the slowly varying pulse envelope, $\beta_1$ is the inverse of the group velocity, $\beta_2$ is the group-velocity dispersion, $\alpha$ is loss, and $\gamma$ is the nonlinear parameter proportional to $n_2$. Note that when $\beta_2 < 0$, the equation allows soliton solutions [42, 43]. Various terms are introduced in this equation to model higher-order effects, of which the most important are third-order dispersion and intrapulse Raman scattering, which can be seen as a delayed nonlinearity.

The equation Eq. (2.22) is known to predict many classical results very well. Due to the presence of terms in both frequency and time domain, it is best evaluated using a so-called split-step Fourier method [9, 44].

Modeling complex quantum systems is generally a much more difficult task compared to classical systems. For multimode quantum systems, the usual approach is to turn to a phase-space representation, typically to the positive-P ($+P$) [45] or Wigner [46] quasiprobability distributions.

The $+P$ distribution evolves according to a corresponding Fokker-Planck equation, which in turn can be translated into a pair of stochastic equations on variables $a$ and $a^\dagger$. These stochastic equations are similar to Eq. (2.22) but with additional noise terms. Using a series of realizations of this equation, we can compute variances of various observables. The exact equations, their derivation, and their application to fibers can be found in [45, 47–51].

For the Wigner distribution, the corresponding equation contains additional higher-order terms, which have to be truncated to allow stochastic modeling. Still, for the initial evolution of bright coherent pulses, the truncated Wigner method gives reliable results. This is usually enough for squeezing in fibers, and this method usually requires significantly fewer trajectories to converge, compared to the $+P$ method [51]. The exact equations, their derivation, and their application to fibers can be found in [47, 50–52].

In this work, the truncated Wigner method is used to support experimental results, as well as to investigate a wider spectrum of possible parameters and materials for designing future experimental setups.

## 2.6 Sensitivity of interferometers

Among various applications of squeezed light states, enhancing interferometer sensitivity is undoubtedly one of the first and one of the most obvious. A very general description of an interferometer can follow a two-rail diagram, as in Fig. 2.4. Here, two states of light $|a_{\text{in}}\rangle$ and $|b_{\text{in}}\rangle$ are mixed at some beamsplitter, then follow different optical paths, where a phase difference $\varphi$ is accumulated. After that, the resulting states are combined again to produce states $|a_{\text{out}}\rangle$ and $|b_{\text{out}}\rangle$, and some measurements are performed on one or both of these states, described with an arbitrary operator $\hat{P}$. Note that the rails $a$ and $b$ do not necessarily represent spatially different modes. For example, they can represent two orthogonal polarization modes; in this case, the beamsplitters are implemented as wave plates.

The mission of an interferometer is to detect changes in $\varphi$, typically around a known value $\varphi_0$. Thus obviously, the stronger the dependence of $\left\langle \hat{P} \right\rangle$ on $\varphi$, the more accurate the measurements. On the other hand,

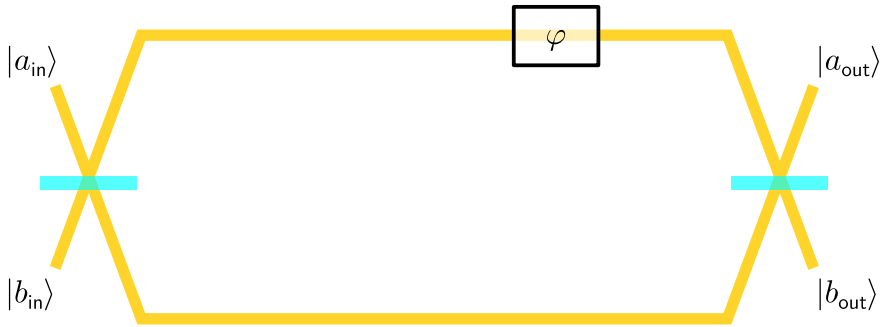


**Figure 2.4:** A general Mach-Zehnder interferometer.

the uncertainty $\Delta P = \left(\left\langle \hat{P}^2 \right\rangle - \left\langle \hat{P} \right\rangle^2\right)^{1/2}$ limits the accuracy, as it is not possible to distinguish two measurements resulting in the values of $P$ within this uncertainty from each other. Thus, the precision of such an interferometer is defined as [53]

$$\Delta\varphi = \frac{\Delta P}{\left|\frac{\partial\langle\hat{P}\rangle}{\partial\varphi}\right|_{\varphi_0}}. \tag{2.23}$$

Here, $\Delta\varphi$ denotes the smallest detectable change in the phase $\varphi$; smaller is more sensitive. Note that in practice, additionally to the quantum uncertainty $\Delta P$, there are classical noises that have to be taken into account.

It is important to note that only the case of low-power light is considered here, in which the classical or quantum state of the interferometer itself is not affected by the light, for example, through heating or by fluctuations of radiation pressure. Such quantum-optomechanical processes could also decrease (or increase, see [54]) the accuracy of an interferometer, however, they are not considered in this thesis.

It turns out that when only coherent light states are used as the input to the interferometer, the resulting precision cannot be smaller than

$$\Delta\varphi^{\text{coh}}_{\text{min}} = \frac{1}{\sqrt{N}}, \tag{2.24}$$

where $N = \langle\hat{n}\rangle_a + \langle\hat{n}\rangle_b$ is the expected total number of photons in the interferometer [55]. However, the ultimate limit on the precision without assumptions on the input quantum states is the Heisenberg limit [56]

$$\Delta\varphi^{\text{H}} = \frac{1}{N}, \tag{2.25}$$

which is obviously much more precise. In order to get closer to this bound, non-coherent states are used at the input of the interferometer.

Caves [55] was the first to show that by launching a coherent state in one input port of the interferometer and a squeezed vacuum in the other port, a better than $N^{-1/2}$ precision scaling is achievable. In this scheme, the precision scaling is $N^{-3/4}$. Various other combinations of input quantum states have been studied theoretically, and for some of them, for example two squeezed non-vacuum states, the scaling of $N^{-1}$ can be reached [53,57].

# Chapter 3

# Robust Kerr squeezing in fibers

## 3.1 Non-polarization squeezing experiments

The first experimental observation of Kerr squeezing in optical fibers [58] was made in 1986. The authors used an additional optical cavity with a sharp phase response to transform the quadrature-squeezed state into an amplitude-squeezed state and observed the reduction of fluctuations in a direct optical power measurement. The noise power was below the SNL by around 0.6 dB. Later, a significant improvement in the squeezing amount [59] was achieved by the use of pulsed light. That greatly increased the peak intensity and, therefore, also the Kerr effect. Consequently, the fiber length required to reach the same effective nonlinear length decreased, reducing the negative effect of unwanted temperature and acoustic phenomena, especially the guided acoustic wave Brillouin scattering (GAWBS). Another improvement was the use of a Sagnac interferometer, in which two pulses propagate simultaneously in the same optical fiber in opposite directions. These pulses are subsequently combined. This idea allows both to reduce the effect of the GAWBS due to its partial self-canceling in the two combined beams and to organize the measurement of an arbitrary quadrature $\hat{X}(\alpha)$ in the phase quadrature space. While in work [58], the fiber had to be Helium-cooled to produce squeezing, in [59], the squeezing of 1.1 dB was already reached at room temperature.

In subsequent works, other different ways were found to transform the Kerr quadrature squeezing into easily-observed amplitude squeezing. In particular, successful approaches include careful adjusting of phases or am-

plitudes of spectral components of the squeezed beam [60–62], or shifting the squeezed ellipse in the phase space using an additional coherent signal [21, 63, 64]. The latter experimental works involve two pulses propagating in the same fiber in opposite directions, and although that reduces the effect of the GAWBS, the pulses pass the same fiber point at different time moments, and therefore the effect of the additional phase noise is not completely canceled. Thus, the next development step was to use two pulses propagating simultaneously in the same fiber in the same direction but in different polarization modes. An earlier approach [65] still used the same idea to combine a quadrature-squeezed state with a coherent state; in this work, a squeezing of 4.4 dB was reached. The negative effect here is that the mixing of a squeezed and a coherent light inevitably reduces the squeezing amount. Later, an improved scheme was introduced, in which both of the pulses that propagate through the fiber in different polarization modes have similar amplitude and experience a similar Kerr effect. This gives two quadrature-squeezed pulses at the output of the fiber [51,66,67]. Analyzing these two states together as one single beam, one notes that this is a polarization-squeezed light state [32, 68], as noted in Section 2.4. In this state, the quantum uncertainty of a particular combination of the Stokes parameters is smaller than that of a coherent state that has the same amplitude and mean polarization. Due to the same propagation direction, the GAWBS affects both pulses similarly, and therefore the effect is suppressed even better. This approach was implemented in the work [67], which currently holds the record of 6.8±0.3 dB observed squeezing obtained in optical fibers using the Kerr effect.

## 3.2 Polarization squeezing via the Kerr effect

Early works connecting Kerr squeezing and Stokes parameters [32,34] only considered uncertainties of $\hat{S}(0) = \hat{S}_1$ and $\hat{S}(\frac{\pi}{2}) = \hat{S}_2$ and overlooked[1] the possibility of squeezing at arbitrary angle $\theta$. The first experimental demonstration of squeezed Stokes parameters was performed in [69] for a $\chi^{(2)}$ medium. In [33], various polarization-squeezed states generated via the Kerr effect were considered; however, their production involved quite complicated setups. Only two years later [66], it was demonstrated that a simple combination of two identical Kerr-squeezed beams in orthogonal polarization modes already produces a polarization-squeezed state that is

[1] In [32] and following, the possibility of squeezing of $\hat{S}_1$ is demonstrated if the two modes experience interaction.

fairly easy to detect. The amplitude-phase correlation introduced by the nonlinearity in each mode is translated into $\hat{S}_1$–$\hat{S}_2$ correlation when both modes are considered together because the $\hat{S}_1$ represents the difference in intensity in the two modes, and $\hat{S}_2$ essentially represents the relative phase of the two modes. Note that a combination of two arbitrary squeezed light states does not guarantee to produce a polarization-squeezed state. It is important that two identically-squeezed states are considered.

The exact orientation of the Kerr-squeezed ellipse on the Poincaré sphere depends on the way the mean polarization state is prepared. When the two independently-squeezed modes are combined, there is a free parameter, the phase difference $\varphi$ of the two states, that can be adjusted. This adjustment moves the mean polarization state along the $S_2$–$S_3$ great circle on the Poincaré sphere while keeping the angle between the axes of the ellipse and the said circle constant (Fig. 3.1). In fact, it is the same angle $\theta_{\mathrm{sq}}$ that we have for the quadrature Kerr squeezing in each mode separately. This way, the uncertainty of $\Delta^2 S_1$, which is the parameter that is the easiest to measure in an experiment, remains constant and equal to that of a coherent state. That could be the reason why this type of squeezing remained unnoticed for some time. However, with simple linear polarization optics, it's possible to align the ellipse so that its minor axis is parallel to the $S_1$ axis, and then the fluctuations are reduced. Exactly this was done in [66] and subsequent works [67, 70] by mixing the modes to produce a circular polarization ($\varphi = \frac{\pi}{2}$) and then rotating the ellipse around the $S_3$ axis with a half-wave plate (Fig. 3.2). Consider a half-wave plate installed such that the angle between its axes and the polarization vectors of the considered modes is $\alpha$. Then, its action in the Poincaré space can be decomposed in two steps: first, a rotation by $\pi$ around $S_1$ that changes the handedness of the circular polarization; then, a rotation by $4\alpha$ around $S_3$. Since polarization handedness is not important in the considered experiments, with the proper choice of $\alpha$, it is possible to align the ellipse properly and observe squeezing.

The work [67] holds the record for squeezing in fibers, achieving an impressive value of $-6.8\,\mathrm{dB}$. This was the measured value; the inferred value in an ideal setup without losses was calculated to be more than $-10\,\mathrm{dB}$. The cited work followed the approach described above, utilizing two polarization modes of a polarization-maintaining fiber to generate two Kerr-squeezed states. To compensate for the group delay difference between the two pulses, a polarizing Michelson interferometer was installed in front of the fiber, giving the pulse launched into the fast axis mode the required de-

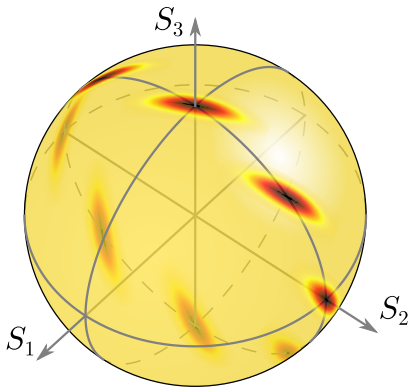


**Figure 3.1:** The possible uncertainty distributions on the Poincaré sphere when the relative phase of the two modes is adjusted.

lay. With the help of the same interferometer and a feedback loop, the mean polarization at the end of the fiber was kept circular. Then, a half-wave plate was used to align the ellipse, as discussed. Even though the experiment proved that converting Kerr squeezing into polarization squeezing is a simple yet reliable and effective approach to produce strong squeezing, still with a sensitive free-space interferometer and an active phase control loop, the setup was rather complicated.

## 3.3 New setup for polarization squeezing generation

Here is where the first part of this thesis comes into view, revising and improving the approach taken in [67]. First, to compensate for the group delay difference, another idea is used. The polarization-maintaining fiber is cut into two parts of equal length and spliced back with a 90° rotation around its axis. This way, the pulse that is polarized along a fast axis in the first half of the fiber is polarized along the slow axis in the second half, and vice versa. The result is that the two pulses arrive at the end of the fiber simultaneously, and there is no more need for a free-space interferometer. Not only this simplified the setup by removing a large element, but it also allowed us to get rid of the feedback loop for phase stabilization because now the two modes always share the same spatial mode, and differential phase fluctuations inside the birefringent fiber are very small.

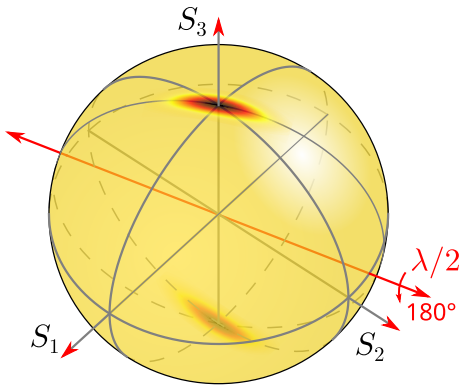


**Figure 3.2:** The action of a half-wave plate on a squeezed circular-polarized state. The squeezed state aligned at some angle to the $S_1$ axis is brought to the opposite pole of the sphere with correct alignment.

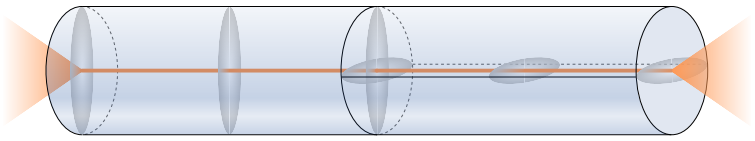

**Figure 3.3:** Structure of the used fiber (not to scale).

Another change was made to the way the circular mean polarization is established. Without the birefringent compensator, the phase difference between the two pulses is not actively controlled at the input of the fiber. It's difficult to cut the fiber with enough precision to ensure equal optical path length even in a linear regime, and given the importance of nonlinear interaction, this should be impossible. Thus, another method should be used to control the polarization. Fortunately, as discussed above, at the end of the fiber, the polarization state would be somewhere on the $S_2$–$S_3$ big circle of the Poincaré sphere, as depicted in Fig. 3.1. Any polarization optic elements can be used to move the state into its correct position; this does not destroy squeezing. In principle, a single birefringent element is enough to bring the ellipse to any position on the sphere with any arbitrary direction of the axes. However, the required eigen polarization modes of this element are, in general, elliptical, and the retardance is, in general, arbitrary. Thus, in this work, instead of a single element, a series of three wave plates are used. First, two quarter-wave plates are used to set the

circular mean polarization (Fig. 3.4). Then, a half-wave plate is used to align the ellipse axes, as discussed above. Note, however, that the angle between the axes and the $S_2$ axis is not necessarily $\theta_{\mathrm{sq}}$ as before but also depends on the ellipticity angle $\chi$ of the initial state.

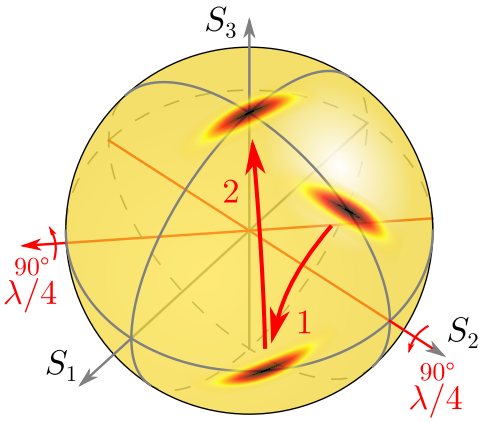


**Figure 3.4:** Producing circularly polarized light using two quarter-wave plates.

The improvements made in this work allowed us to assemble two simple and very stable setups that deliver more than $-5\,\mathrm{dB}$ of squeezing. The setups operated in a laboratory environment at room temperature for long periods of time. Squeezing decayed on the timescale of several days due to various environmental changes. The details of these setups and obtained results are published in the following article.

- Kalinin, N., Dirmeier, T., Sorokin, A. A., Anashkina, E. A., Sánchez-Soto, L. L., Corney, J. F., Leuchs, G., Andrianov, A. V., Observation of Robust Polarization Squeezing via the Kerr Nonlinearity in an Optical Fiber.
  Adv Quantum Technol. 6, 2200143, 2023. 10.1002/qute.202200143.

## 3.4 Future improvements

The novel experimental setup demonstrated in this work, despite being significantly easier, does not beat the current squeezing record in fibers [67] at this time. This could be attributed to a number of factors, such as non-negligible losses, suboptimal fiber length and pulse duration values. In

order to reach the best possible squeezing in silica fibers, a numerical search in an extended three-dimensional parameter space was performed using the model described in Section 2.5. The results of this work are presented in the following article.

- Andrianov, A. V., Kalinin, N. A., Sorokin, A. A., Anashkina, E. A., Sánchez-Soto, L. L., Corney, J. F., and Leuchs, G., Optimizing the generation of polarization squeezed light in nonlinear optical fibers driven by femtosecond pulses, Opt. Express 31, 765, 2023. 10.1364/OE.481195.

These include a comparison with a couple of data points from an experimental setup with increased fiber length, which is being investigated now. These points already show squeezing of more than 5.5 dB, and the simulation predicts that even better results could be achieved.

Additional research is performed on new fiber materials, such as tellurite and chalcogenide glasses. The choice of these two glasses is supported by two reasons. First, the nonlinearity in these media is much stronger than in silica [71, 72], which allows using shorter pieces of fiber to achieve the same squeezing levels. This, in turn, reduces the negative effects of Raman and Brillouin scattering and also reduces losses. Second, these glasses have much lower losses around 2 µm wavelengths, which might be crucial to future generations of gravitational wave detectors [73, 74].

Recently, squeezing in the 2 µm wavelength region has been demonstrated using $\chi^{(2)}$ nonlinearity [75–77]. However, so far, there hasn't been any demonstration of squeezing generated in fibers above the 1.55 µm wavelength region. Nevertheless, as soft-glass fibers appear more and more often in laboratories, and some are already available on the market, there is no doubt that squeezing experiments will follow. In order to provide better insight into the optimal parameters of future setups, and possible results, a series of numerical experiments have been performed for chalcogenide and tellurite glass fibers. The results are published in the following article.

- Sorokin, A. A., Leuchs, G., Corney, J. F., Kalinin, N. A., Anashkina, E. A., and Andrianov, A. V., Towards Quantum Noise Squeezing for 2-Micron Light with Tellurite and Chalcogenide Fibers with Large Kerr Nonlinearity, Mathematics, 10 (19), 3477, 2022. 10.3390/math10193477.

The modeling demonstrated that soft glass fibers can provide significant levels of squeezing, which are unreachable for silica fibers for the used wavelengths. Using realistic fiber parameters, we predicted squeezing of more

than $-15\,\mathrm{dB}$ for fiber lengths shorter than $1\,\mathrm{m}$. Although in experiments these high values would be hard to achieve due to additional losses and unaccounted phase noise, still, the results are very promising.

# Chapter 4

# Phase sensitivity enhancement in interferometers

## 4.1 Squeezing-enhanced interferometry using squeezed vacuum

In Section 2.6, we discussed different approaches to enhancing interferometry sensitivity using squeezed light states and theoretical bounds. Yet in experiments so far, it is not the theoretical scaling that limits the precision but rather the available degree of squeezing, the possibility of applying certain states to interferometry, as well as the losses inside the interferometer and the detection scheme. Essentially, only the first scheme originally suggested by Caves is used. Replacing coherent vacuum input to the dark port (i. e., the default situation) with a squeezed vacuum is fairly straightforward for applications, including the most demanding gravitational forces measurements. The first demonstrations were done in [78, 79]. Works [80–82] extended prototype interferometers to various elements of large-scale gravitational-wave detectors, such as power recycling, signal recycling, and large-scale suspended mirrors. Subsequently, the largest detectors started using squeezed vacuum as an instrument to enhance their sensitivity on an everyday basis. Currently, the typical signal-to-noise ratio (SNR) enhancement are 3.2 dB in the Advanced Virgo detector, and 6 dB in the GEO 600 detector [4, 83]. In table-top experiments, however, much better values of more than 10 dB have been reported recently [8, 84]. In all

these experiments, $\chi^{(2)}$ nonlinearity has been used to produce the squeezed vacuum.

## 4.2 Tilting of Kerr ellipse and interferometry

The tilting of the uncertainty ellipse obtained in Kerr squeezing (and subsequent polarization squeezing) prevents their straightforward usage in phase-sensitive interferometers. In order to observe Kerr squeezing, an interferometer is required with light in one or both arms undergoing nonlinear self-interaction. On the beamsplitter at the end of the interferometer, the squeezed quadratures are projected onto the measuring axes, and thus the noise reduction is visible. However, this interferometer itself does not provide enhanced sensitivity. This is because in order to observe SNR enhancement, not only the measurement variable must be aligned with the squeezed axis of the uncertainty ellipse, but also the signal to be measured should shift the squeezed ellipse along its minor axis. This is not possible in a standard interferometer shown in Fig. 2.4. It was already noted in 1991 [85] that by separating the squeezer interferometer and the sensor interferometer with a certain basis change, one can go below the shot noise limit with $\chi^{(3)}$ nonlinearity. However, this theory paper has been largely unnoticed, and no experiment was made. It should be noted that recently Kerr squeezing has been successfully used in sub-SNL transmission estimation [86].

Meanwhile, in a related field of atom interferometry, a similar problem existed. Ramsey spectroscopy, the state-of-the-art method to measure time, is a direct analog to optical interferometry. Moreover, the technique called "one axis twisting" allows reliable and fast creation of squeezed states [87]; however, on the Bloch sphere, which is the atom equivalent to the Poincaré sphere, the squeezed state is a tilted ellipse, much like a Kerr-squeezed state in optics. In order to decrease uncertainty in measurements, the squeezed state has to be rotated accordingly, which was understood and implemented by several groups [88–90]. The alignment of the uncertainty ellipse here was performed using several pulses with carefully chosen area and phase. This allowed Ramsey spectroscopy to go below the SNL; however, no direct link to the Kerr squeezing was made.

## 4.3 Kerr-squeezed interferometer

In this work, we came up with a way to apply polarization squeezing obtained via the Kerr effect to an interferometer to enhance its phase sensitivity and built an experimental setup demonstrating 4 dB SNR enhancement. The idea is, after preparing the polarization-squeezed state, to rotate the uncertainty ellipse on the Poincaré sphere so that its minor axis is aligned both with the movements introduced by the changes of the measured phase $\varphi$ and with the measurement axis. This requires separating the interferometer into two parts. In the first part, the squeezed state is prepared, while the second part is phase-sensitive with a basis change between them (Fig. 4.1). The proper alignment of the squeezed ellipse between the parts is done with waveplates, as shown in Fig. 3.4.

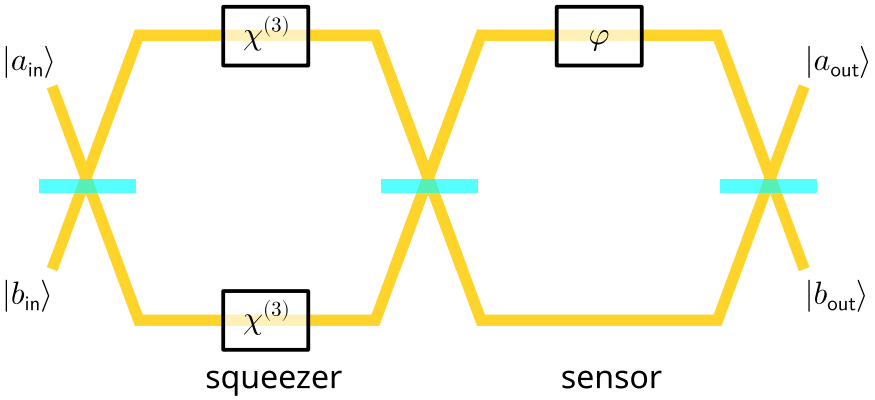


**Figure 4.1:** The scheme of a Kerr-squeezed interferometer. In the squeezer part, the squeezed state is prepared, while in the sensor part, the signal is introduced.

The details and results are published in the following article.

- Kalinin, N., Dirmeier, T., Sorokin, A. A., Anashkina, E. A., Sánchez-Soto, L. L., Corney, J. F., Leuchs, G., Andrianov, A. V., Quantum-enhanced interferometer using Kerr squeezing. Nanophotonics 12 (14), 2945, 2023. 10.1515/nanoph-2023-0032.

To the best of our knowledge, this is the first experimental demonstration of sub-SNL phase measurements using Kerr squeezing. Although the SNR improvement is still smaller than in the best experiments with $\chi^{(2)}$

nonlinearity, it is already good enough to be used in real-world applications. Especially in setups with significant losses, further improvements in SNR enhancement are useless. We hope that when better sources of Kerr squeezing are created, for example, using non-silica fibers, Kerr-squeezing-enhanced interferometry may be notably improved, similar to the path "coherent+squeezed vacuum" interferometry took in the last 35 years.

# Chapter 5

# Conclusion and outlook

This thesis is devoted to squeezed states of light produced by the Kerr effect in optical fibers. While an optical fiber is a relatively simple system, its use as a medium for the generation of non-classical states is still not yet fully explored. This work contains two results that advance this field and hopefully can be useful for future applications: a novel, simple all-fiber setup for squeezed light generation and a method to apply Kerr-squeezed states to enhance interferometric sensitivity beyond the shot-noise limit.

In [91], we present an improved scheme to generate polarization-squeezed states using a polarization-maintaining fiber. The suggested approach uses only passive elements and thus is extremely robust. Implemented experimental setups delivered more than $-5\,\mathrm{dB}$ of squeezing during prolonged runs without any need for adjustments. This demonstrated the reliability and stability of the proposed approach.

Even though the current results do not surpass the known record of squeezing in fibers, our simulations (see [92]) show that this result is within reach with the proper choice of parameters. Our current work is focused on exploring the space of possible parameters to find those optimal for strong squeezing generation. Additionally, an interesting approach that is currently being investigated is the use of other fiber materials (see [93]) to create a compact and stable source of squeezed light in a longer wavelength range.

In [94], the first Kerr-squeezed phase interferometer with sensitivity below the shot-noise limit is demonstrated. The key idea that allowed us to make use of the Kerr-squeezed uncertainty ellipse was to split the interferometer into the squeezer and sensor parts and introduce a basis change between them. In our experiment, the signal-to-noise ratio improvement

was 4 dB compared to the use of a coherent state. The improvement was limited by the available squeezing and additional losses introduced in the sensing part of the interferometer setup.

The demonstrated sub-SNL interferometer operates at an eye-safe wavelength, uses a very robust source of squeezing, and does not require mode-matching of multiple sources, in contrast to traditional sub-SNL interferometers that utilize squeezed vacuum. All of this should be very beneficial for future applications. Our future research in this direction would be first focused on improving the squeezing source as described above and also on demonstrating the sub-SNL free-space interferometer based on the proposed principle.

# Bibliography


[1] R. J. Glauber, "Coherent and incoherent states of the radiation field," *Phys. Rev.*, vol. 131, pp. 2766–2788, 1963. https://doi.org/10.1103/PhysRev.131.2766

[2] D. F. Walls, "Squeezed states of light," *Nature*, vol. 306, no. 5939, pp. 141–146, 1983. https://doi.org/10.1038/306141a0

[3] R. E. Slusher, L. W. Hollberg, B. Yurke, J. C. Mertz, and J. F. Valley, "Observation of squeezed states generated by four-wave mixing in an optical cavity," *Phys. Rev. Lett.*, vol. 55, pp. 2409–2412, 1985. https://doi.org/10.1103/PhysRevLett.55.2409

[4] F. Acernese, M. Agathos, L. Aiello, et al., "Increasing the astrophysical reach of the Advanced Virgo detector via the application of squeezed vacuum states of light," *Phys. Rev. Lett.*, vol. 123, p. 231108, 2019. https://doi.org/10.1103/PhysRevLett.123.231108

[5] H.-S. Zhong, H. Wang, Y.-H. Deng, et al., "Quantum computational advantage using photons," *Science*, vol. 370, no. 6523, pp. 1460–1463, 2020. https://doi.org/10.1126/science.abe8770

[6] U. L. Andersen, T. Gehring, C. Marquardt, and G. Leuchs, "30 years of squeezed light generation," *Physica Scripta*, vol. 91, p. 053001, 2016. https://doi.org/10.1088/0031-8949/91/5/053001

[7] R. Nehra, R. Sekine, L. Ledezma, et al., "Few-cycle vacuum squeezing in nanophotonics," *Science*, vol. 377, no. 6612, pp. 1333–1337, 2022. https://doi.org/10.1126/science.abo6213

[8] J. Zander, C. Rembe, and R. Schnabel, "10 dB interferometer enhancement by squeezing of photon shot noise with sub-femtometer resolution and eye-safe optical power," *Quantum Sci. Technol.*, vol. 8, p. 01LT01, 2022. https://doi.org/10.1088/2058-9565/ac9ad5

[9] G. P. Agrawal, *Nonlinear fiber optics*. Amsterdam, Elsevier/Academic Press, fifth edition ed., 2013.

[10] S. Machida, Y. Yamamoto, and Y. Itaya, "Observation of amplitude squeezing in a constant-current–driven semiconductor laser," *Phys. Rev. Lett.*, vol. 58, pp. 1000–1003, 1987. https://doi.org/10.1103/PhysRevLett.58.1000

[11] T. C. Ralph and C. M. Savage, "Squeezed light from conventionally pumped multilevel lasers," *Opt. Lett.*, vol. 16, pp. 1113–1115, 1991. https://doi.org/10.1364/OL.16.001113

[12] C. M. Caves, "Amplitude and phase in quantum optics," in: F. Haake, L. M. Narducci, and D. F. Walls (eds.), *Coherence, cooperation and fluctuations*, Cambridge University Press, 1985.

[13] H.-A. Bachor and T. C. Ralph, "A guide to experiments in quantum optics," in: *A Guide to Experiments in Quantum Optics*, third ed., John Wiley & Sons, Ltd, 2019.

[14] A. Royer, "Wigner function as the expectation value of a parity operator," *Phys. Rev. A*, vol. 15, pp. 449–450, 1977. https://doi.org/10.1103/PhysRevA.15.449

[15] T. Tilma, M. J. Everitt, J. H. Samson, W. J. Munro, and K. Nemoto, "Wigner functions for arbitrary quantum systems," *Phys. Rev. Lett.*, vol. 117, p. 180401, 2016. https://doi.org/10.1103/PhysRevLett.117.180401

[16] U. Seyfarth, A. B. Klimov, H. d. Guise, G. Leuchs, and L. L. Sanchez-Soto, "Wigner function for SU(1,1)," *Quantum*, vol. 4, p. 317, 2020. https://doi.org/10.22331/q-2020-09-07-317

[17] R. Slusher and B. Yurke, "Squeezed light for coherent communications," *Journal of Lightwave Technology*, vol. 8, no. 3, pp. 466–477, 1990. https://doi.org/10.1109/50.50742

[18] M. Gu, C. Weedbrook, N. C. Menicucci, T. C. Ralph, and P. van Loock, "Quantum computing with continuous-variable clusters," *Phys. Rev. A*, vol. 79, p. 062318, 2009. https://doi.org/10.1103/PhysRevA.79.062318

[19] S. Pirandola, S. Mancini, S. Lloyd, and S. L. Braunstein, "Continuous-variable quantum cryptography using two-way quantum communication," *Nature Physics*, vol. 4, no. 9, pp. 726–730, 2008.

[20] L.-A. Wu, H. J. Kimble, J. L. Hall, and H. Wu, "Generation of squeezed states by parametric down conversion," *Phys. Rev. Lett.*, vol. 57, pp. 2520–2523, 1986. https://doi.org/10.1103/PhysRevLett.57.2520

[21] M. Kitagawa and Y. Yamamoto, "Number-phase minimum-uncertainty state with reduced number uncertainty in a Kerr nonlinear interferometer," *Phys. Rev. A*, vol. 34, pp. 3974–3988, 1986. https://doi.org/10.1103/PhysRevA.34.3974

[22] R. Tanaś and S. Kielich, "Self-squeezing of light propagating through nonlinear optically isotropic media," *Optics Communications*, vol. 45, no. 5, pp. 351–356, 1983. https://doi.org/10.1016/0030-4018(83)90264-X

[23] R. Tanas, "Nonclassical states of light propagating in Kerr media," *Theory of Nonclassical States of Light*, p. 277, 2003.

[24] M. Stobińska, G. J. Milburn, and K. Wódkiewicz, "Wigner function evolution of quantum states in the presence of self-Kerr interaction," *Phys. Rev. A*, vol. 78, p. 013810, 2008. https://doi.org/10.1103/PhysRevA.78.013810

[25] B. L. Schumaker, "Noise in homodyne detection," *Opt. Lett.*, vol. 9, pp. 189–191, 1984. https://doi.org/10.1364/OL.9.000189

[26] A. S. Villar, "The conversion of phase to amplitude fluctuations of a light beam by an optical cavity," *Am. J. Phys.*, vol. 76, no. 10, pp. 922–929, 2008. https://doi.org/10.1119/1.2937903

[27] P. Galatola, L. Lugiato, M. Porreca, P. Tombesi, and G. Leuchs, "System control by variation of the squeezing phase," *Opt. Commun.*, vol. 85, no. 1, pp. 95–103, 1991. https://doi.org/10.1016/0030-4018(91)90056-J

[28] C. C. Gerry and R. Grobe, "Statistical properties of squeezed Kerr states," *Phys. Rev. A*, vol. 49, pp. 2033–2039, 1994. https://doi.org/10.1103/PhysRevA.49.2033

[29] K. Sundar, "Highly amplitude-squeezed states of the radiation field," *Phys. Rev. Lett.*, vol. 75, pp. 2116–2119, 1995. https://doi.org/10.1103/PhysRevLett.75.2116

[30] A. D. Wilson-Gordon, V. Buek, and P. L. Knight, "Statistical and phase properties of displaced Kerr states," *Phys. Rev. A*, vol. 44, pp. 7647–7656, 1991. https://doi.org/10.1103/PhysRevA.44.7647

[31] M. Shirasaki and H. A. Haus, "Squeezing of pulses in a nonlinear interferometer," *J. Opt. Soc. Am. B*, vol. 7, pp. 30–34, 1990. https://doi.org/10.1364/JOSAB.7.000030

[32] A. S. Chirkin, A. A. Orlov, and D. Y. Parashchuk, "Quantum theory of two-mode interactions in optically anisotropic media with cubic nonlinearities: Generation of quadrature- and polarization-squeezed light," *Quantum Elect.*, vol. 23, pp. 870–874, 1993. https://doi.org/10.1070/qe1993v023n10abeh003182

[33] J. Heersink, T. Gaber, S. Lorenz, O. Glöckl, N. Korolkova, and G. Leuchs, "Polarization squeezing of intense pulses with a fiber-optic Sagnac interferometer," *Phys. Rev. A*, vol. 68, p. 013815, 2003. https://doi.org/10.1103/PhysRevA.68.013815

[34] R. Tanaś and S. Kielich, "Quantum fluctuations in the Stokes parameters of light propagating in a Kerr medium," *Journal of Modern Optics*, vol. 37, no. 12, pp. 1935–1945, 1990. https://doi.org/10.1080/09500349014552141

[35] N. Korolkova, G. Leuchs, R. Loudon, T. C. Ralph, and C. Silberhorn, "Polarization squeezing and continuous-variable polarization entanglement," *Phys. Rev. A*, vol. 65, p. 052306, 2002. https://doi.org/10.1103/PhysRevA.65.052306

[36] G. G. Stokes, "On the perfect blackness of the central spot in Newton's rings, and on the verification of Fresnel's formulae for the intensities of reflected and refracted rays," *Cambridge and Dublin Math. J.*, vol. IV, p. 1, 1849.

[37] A. Z. Goldberg, P. de la Hoz, G. Björk, et al., "Quantum concepts in optical polarization," *Adv. Opt. Photon.*, vol. 13, pp. 1–73, 2021. https://doi.org/10.1364/AOP.404175

[38] C. Silberhorn, P. K. Lam, O. Weiß, F. König, N. Korolkova, and G. Leuchs, "Generation of continuous variable Einstein-Podolsky-Rosen entanglement via the Kerr nonlinearity in an optical fiber," *Phys. Rev. Lett.*, vol. 86, pp. 4267–4270, 2001. https://doi.org/10.1103/PhysRevLett.86.4267

[39] M. D. Reid, P. D. Drummond, W. P. Bowen, et al., "Colloquium: The Einstein-Podolsky-Rosen paradox: From concepts to applications," *Rev. Mod. Phys.*, vol. 81, pp. 1727–1751, 2009. https://doi.org/10.1103/RevModPhys.81.1727

[40] E. Arthurs and J. L. Kelly, "On the simultaneous measurement of a pair of conjugate observables," *Bell Syst. Tech. J.*, vol. 44, no. 4, pp. 725–729, 1965. https://doi.org/10.1002/j.1538-7305.1965.tb01684.x

[41] S. Stenholm, "Simultaneous measurement of conjugate variables," *Ann. Phys.*, vol. 218, no. 2, pp. 233–254, 1992. https://doi.org/10.1016/0003-4916(92)90086-2

[42] J. S. Russel, "Report on waves, 14th Mtg. of the British Assoc. for the Advance of Science," 1844.

[43] A. Shabat and V. Zakharov, "Exact theory of two-dimensional self-focusing and one-dimensional self-modulation of waves in nonlinear media," *Sov. Phys. JETP*, vol. 34, no. 1, p. 62, 1972.

[44] R. A. Fisher and W. K. Bischel, "Numerical studies of the interplay between self-phase modulation and dispersion for intense plane-wave laser pulses," *Journal of Applied Physics*, vol. 46, pp. 4921–4934, 1975. https://doi.org/10.1063/1.321476

[45] P. D. Drummond and C. W. Gardiner, "Generalised P-representations in quantum optics," *Journal of Physics A: Mathematical and General*, vol. 13, p. 2353, 1980. https://doi.org/10.1088/0305-4470/13/7/018

[46] E. Wigner, "On the quantum correction for thermodynamic equilibrium," *Physical Review*, vol. 40, no. 5, p. 749 – 759, 1932. https://doi.org/10.1103/PhysRev.40.749 Cited by: 7498.

[47] S. J. Carter, "Quantum theory of nonlinear fiber optics: Phase-space representations," *Phys. Rev. A*, vol. 51, pp. 3274–3301, 1995. https://doi.org/10.1103/PhysRevA.51.3274

[48] P. D. Drummond and S. J. Carter, "Quantum-field theory of squeezing in solitons," *J. Opt. Soc. Am. B*, vol. 4, pp. 1565–1573, 1987. https://doi.org/10.1364/JOSAB.4.001565

[49] S. J. Carter and P. D. Drummond, "Squeezed quantum solitons and raman noise," *Phys. Rev. Lett.*, vol. 67, pp. 3757–3760, 1991. https://doi.org/10.1103/PhysRevLett.67.3757

[50] P. D. Drummond and J. F. Corney, "Quantum noise in optical fibers. I. Stochastic equations," *J. Opt. Soc. Am. B*, vol. 18, pp. 139–152, 2001. https://doi.org/10.1364/JOSAB.18.000139

[51] J. F. Corney, J. Heersink, R. Dong, et al., "Simulations and experiments on polarization squeezing in optical fiber," *Phys. Rev. A*, vol. 78, p. 023831, 2008. https://doi.org/10.1103/PhysRevA.78.023831

[52] P. D. Drummond and A. D. Hardman, "Simulation of quantum effects in Raman-active waveguides," *Europhysics Letters*, vol. 21, p. 279, 1993. https://doi.org/10.1209/0295-5075/21/3/005

[53] R. Demkowicz-Dobrzański, M. Jarzyna, and J. Kołodyński, "Quantum limits in optical interferometry," *Progress in Optics*, vol. 60, pp. 345–435, 2015. https://doi.org/10.1016/bs.po.2015.02.003

[54] H. J. Kimble, Y. Levin, A. B. Matsko, K. S. Thorne, and S. P. Vyatchanin, "Conversion of conventional gravitational-wave interferometers into quantum nondemolition interferometers by modifying their input and/or output optics," *Phys. Rev. D*, vol. 65, p. 022002, 2001. https://doi.org/10.1103/PhysRevD.65.022002

[55] C. M. Caves, "Quantum-mechanical noise in an interferometer," *Phys. Rev. D*, vol. 23, pp. 1693–1708, 1981. https://doi.org/10.1103/PhysRevD.23.1693

[56] Z. Y. Ou, "Fundamental quantum limit in precision phase measurement," *Phys. Rev. A*, vol. 55, pp. 2598–2609, 1997. https://doi.org/10.1103/PhysRevA.55.2598

[57] D. Bruss and G. Leuchs, *Lectures on Quantum Information*. Physics textbook, Wiley, 2007.

[58] R. M. Shelby, M. D. Levenson, S. H. Perlmutter, R. G. DeVoe, and D. F. Walls, "Broad-band parametric deamplification of quantum noise

in an optical fiber," *Phys. Rev. Lett.*, vol. 57, pp. 691–694, 1986. https://doi.org/10.1103/PhysRevLett.57.691

[59] M. Rosenbluh and R. M. Shelby, "Squeezed optical solitons," *Phys. Rev. Lett.*, vol. 66, pp. 153–156, 1991. https://doi.org/10.1103/PhysRevLett.66.153

[60] S. R. Friberg, S. Machida, M. J. Werner, A. Levanon, and T. Mukai, "Observation of optical soliton photon-number squeezing," *Phys. Rev. Lett.*, vol. 77, pp. 3775–3778, 1996. https://doi.org/10.1103/PhysRevLett.77.3775

[61] S. Spälter, N. Korolkova, F. König, A. Sizmann, and G. Leuchs, "Observation of multimode quantum correlations in fiber optical solitons," *Phys. Rev. Lett.*, vol. 81, no. 4, p. 786, 1998.

[62] E. H. Huntington, G. N. Milford, C. Robilliard, et al., "Demonstration of the spatial separation of the entangled quantum sidebands of an optical field," *Phys. Rev. A*, vol. 71, p. 041802, 2005. https://doi.org/10.1103/PhysRevA.71.041802

[63] S. Schmitt, J. Ficker, M. Wolff, F. König, A. Sizmann, and G. Leuchs, "Photon-number squeezed solitons from an asymmetric fiber-optic Sagnac interferometer," *Phys. Rev. Lett.*, vol. 81, no. 12, p. 2446, 1998.

[64] D. Krylov and K. Bergman, "Amplitude-squeezed solitons from an asymmetric fiber interferometer," *Opt. Lett.*, vol. 23, pp. 1390–1392, 1998. https://doi.org/10.1364/OL.23.001390

[65] M. Fiorentino, J. E. Sharping, P. Kumar, D. Levandovsky, and M. Vasilyev, "Soliton squeezing in a Mach-Zehnder fiber interferometer," *Phys. Rev. A*, vol. 64, p. 031801, 2001. https://doi.org/10.1103/PhysRevA.64.031801

[66] J. Heersink, V. Josse, G. Leuchs, and U. L. Andersen, "Efficient polarization squeezing in optical fibers," *Opt. Lett.*, vol. 30, pp. 1192–1194, 2005. https://doi.org/10.1364/OL.30.001192

[67] R. Dong, J. Heersink, J. F. Corney, P. D. Drummond, U. L. Andersen, and G. Leuchs, "Experimental evidence for Raman-induced limits to efficient squeezing in optical fibers," *Opt. Lett.*, vol. 33, no. 2, pp. 116–118, 2008.

[68] C. R. Müller, B. Stoklasa, C. Peuntinger, et al., "Quantum polarization tomography of bright squeezed light," *New Journal of Physics*, vol. 14, p. 085002, 2012. https://doi.org/10.1088/1367-2630/14/8/085002

[69] J. Hald, J. L. S rensen, C. Schori, and E. S. Polzik, "Entanglement transfer from light to atoms," *Journal of Modern Optics*, vol. 47, no. 14-15, pp. 2599–2614, 2000. https://doi.org/10.1080/09500340008232184

[70] A. Hosaka, K. Hirosawa, R. Sawada, and F. Kannari, "Generation of photon-number squeezed states with a fiber-optic symmetric interferometer," *Opt. Express*, vol. 23, pp. 18850–18863, 2015. https://doi.org/10.1364/OE.23.018850

[71] A. Lin, A. Zhang, E. J. Bushong, and J. Toulouse, "Solid-core tellurite glass fiber for infrared and nonlinear applications," *Opt. Express*, vol. 17, pp. 16716–16721, 2009. https://doi.org/10.1364/OE.17.016716

[72] J. S. Sanghera, L. B. Shaw, P. Pureza, et al., "Nonlinear properties of chalcogenide glass fibers," *International Journal of Applied Glass Science*, vol. 1, no. 3, pp. 296–308, 2010. https://doi.org/10.1111/j.2041-1294.2010.00021.x

[73] J. Steinlechner, I. W. Martin, A. S. Bell, et al., "Silicon-based optical mirror coatings for ultrahigh precision metrology and sensing," *Phys. Rev. Lett.*, vol. 120, p. 263602, 2018. https://doi.org/10.1103/PhysRevLett.120.263602

[74] LIGO Scientific Collaboration, "Instrument science white paper," *LIGO Document: LIGO-T1400316*, 2015.

[75] G. L. Mansell, T. G. McRae, P. A. Altin, et al., "Observation of squeezed light in the 2 $\mu$m region," *Phys. Rev. Lett.*, vol. 120, p. 203603, 2018. https://doi.org/10.1103/PhysRevLett.120.203603

[76] M. J. Yap, D. W. Gould, T. G. McRae, et al., "Squeezed vacuum phase control at 2 $\mu$m," *Opt. Lett.*, vol. 44, pp. 5386–5389, 2019. https://doi.org/10.1364/OL.44.005386

[77] C. Darsow-Fromm, J. Gurs, R. Schnabel, and S. Steinlechner, "Squeezed light at 2128 nm for future gravitational-wave observatories," *Opt. Lett.*, vol. 46, pp. 5850–5853, 2021. https://doi.org/10.1364/OL.433878

[78] M. Xiao, L.-A. Wu, and H. J. Kimble, "Precision measurement beyond the shot-noise limit," *Phys. Rev. Lett.*, vol. 59, pp. 278–281, 1987. https://doi.org/10.1103/PhysRevLett.59.278

[79] P. Grangier, R. E. Slusher, B. Yurke, and A. LaPorta, "Squeezed-light–enhanced polarization interferometer," *Phys. Rev. Lett.*, vol. 59, pp. 2153–2156, 1987. https://doi.org/10.1103/PhysRevLett.59.2153

[80] K. McKenzie, D. A. Shaddock, D. E. McClelland, B. C. Buchler, and P. K. Lam, "Experimental demonstration of a squeezing-enhanced power-recycled michelson interferometer for gravitational wave detection," *Phys. Rev. Lett.*, vol. 88, p. 231102, 2002. https://doi.org/10.1103/PhysRevLett.88.231102

[81] H. Vahlbruch, S. Chelkowski, B. Hage, A. Franzen, K. Danzmann, and R. Schnabel, "Demonstration of a squeezed-light-enhanced power- and signal-recycled Michelson interferometer," *Phys. Rev. Lett.*, vol. 95, p. 211102, 2005. https://doi.org/10.1103/PhysRevLett.95.211102

[82] K. Goda, O. Miyakawa, E. E. Mikhailov, et al., "A quantum-enhanced prototype gravitational-wave detector," *Nat. Phys.*, vol. 4, no. 6, pp. 472–476, 2008.

[83] J. Lough, E. Schreiber, F. Bergamin, et al., "First demonstration of 6 dB quantum noise reduction in a kilometer scale gravitational wave observatory," *Phys. Rev. Lett.*, vol. 126, p. 041102, 2021. https://doi.org/10.1103/PhysRevLett.126.041102

[84] J. Heinze, K. Danzmann, B. Willke, and H. Vahlbruch, "10 dB quantum-enhanced Michelson interferometer with balanced homodyne detection," *Phys. Rev. Lett.*, vol. 129, p. 031101, 2022. https://doi.org/10.1103/PhysRevLett.129.031101

[85] M. Shirasaki, "Quantum-noise reduction in a phase-sensitive interferometer using nonclassical light produced through Kerr media," *Opt.*

*Lett.*, vol. 16, pp. 171–173, 1991. https://doi.org/10.1364/OL.16.000171

[86] G. Atkinson, E. Allen, G. Ferranti, A. McMillan, and J. Matthews, "Quantum enhanced precision estimation of transmission with bright squeezed light," *Phys. Rev. Appl.*, vol. 16, p. 044031, 2021. https://doi.org/10.1103/PhysRevApplied.16.044031

[87] G.-R. Jin, Y.-C. Liu, and W.-M. Liu, "Spin squeezing in a generalized one-axis twisting model," *New Journal of Physics*, vol. 11, p. 073049, 2009. https://doi.org/10.1088/1367-2630/11/7/073049

[88] C. Gross, T. Zibold, E. Nicklas, J. Estève, and M. K. Oberthaler, "Nonlinear atom interferometer surpasses classical precision limit," *Nature*, vol. 464, no. 7292, pp. 1165–1169, 2010. https://doi.org/10.1038/nature08919

[89] O. Hosten, N. J. Engelsen, R. Krishnakumar, and M. A. Kasevich, "Measurement noise 100 times lower than the quantum-projection limit using entangled atoms," *Nature*, vol. 529, no. 7587, pp. 505–508, 2016.

[90] A. Chu, P. He, J. K. Thompson, and A. M. Rey, "Quantum enhanced cavity QED interferometer with partially delocalized atoms in lattices," *Phys. Rev. Lett.*, vol. 127, p. 210401, 2021. https://doi.org/10.1103/PhysRevLett.127.210401

[91] N. Kalinin, T. Dirmeier, A. A. Sorokin, et al., "Observation of robust polarization squeezing via the Kerr nonlinearity in an optical fiber," *Advanced Quantum Technologies*, vol. 6, no. n/a, p. 2200143, 2023. https://doi.org/10.1002/qute.202200143

[92] A. V. Andrianov, N. A. Kalinin, A. A. Sorokin, et al., "Optimizing the generation of polarization squeezed light in nonlinear optical fibers driven by femtosecond pulses," *Opt. Express*, vol. 31, pp. 765–773, 2023. https://doi.org/10.1364/OE.481195

[93] A. A. Sorokin, G. Leuchs, J. F. Corney, N. A. Kalinin, E. A. Anashkina, and A. V. Andrianov, "Towards quantum noise squeezing for 2-micron light with tellurite and chalcogenide fibers with large Kerr nonlinearity," *Mathematics*, vol. 10, no. 19, 2022. https://doi.org/10.3390/math10193477

[94] N. Kalinin, T. Dirmeier, A. A. Sorokin, et al., "Quantum-enhanced interferometer using Kerr squeezing," *Nanophotonics*, vol. 12, no. 14, pp. 2945–2952, 2023. https://doi.org/doi:10.1515/nanoph-2023-0032

# Part II

# Publications

The publications listed below are part of this thesis. They can be openly accessed via the respective journals. Due to legal reasons, they are not published here.

- Kalinin, N., Dirmeier, T., Sorokin, A. A., Anashkina, E. A., Sánchez-Soto, L. L., Corney, J. F., Leuchs, G., Andrianov, A. V., Observation of Robust Polarization Squeezing via the Kerr Nonlinearity in an Optical Fiber.
  Adv Quantum Technol. 6, 2200143, 2023. 10.1002/qute.202200143.

- Andrianov, A. V., Kalinin, N. A., Sorokin, A. A., Anashkina, E. A., Sánchez-Soto, L. L., Corney, J. F., and Leuchs, G.,
  Optimizing the generation of polarization squeezed light in nonlinear optical fibers driven by femtosecond pulses,
  Opt. Express 31, 765, 2023. 10.1364/OE.481195.

- Sorokin, A. A., Leuchs, G., Corney, J. F., Kalinin, N. A., Anashkina, E. A., and Andrianov, A. V.,
  Towards Quantum Noise Squeezing for 2-Micron Light with Tellurite and Chalcogenide Fibers with Large Kerr Nonlinearity,
  Mathematics 10 (19), 3477, 2022. 10.3390/math10193477.

- Kalinin, N., Dirmeier, T., Sorokin, A. A., Anashkina, E. A., Sánchez-Soto, L. L., Corney, J. F., Leuchs, G., Andrianov, A. V., Quantum-enhanced interferometer using Kerr squeezing.
  Nanophotonics 12 (14), 2945, 2023. 10.1515/nanoph-2023-0032.